Development of Two-Degree-of-Freedom Control for Robot Manipulator with Biarticular Muscle Torque

Sehoon Oh and Yoichi Hori

Abstract— This paper suggests control algorithm for a robot manipulator which has biarticular muscle torque input in addition to the conventional two monoarticular muscle torques. Using a modified Jacobian matrix which is based on the absolute angle of two joints, we derive simple relationship between an endpoint force/position and three muscle torques. Based on this relationship a feedback controller is developed to design endpoint stiffness. The proposed control realizes the endpoint stiffness with arbitrary major axis, minor axis, and tilt angle with simple gain decision. As for the feedforward control, the dynamics of three muscles torque are derived and used as inverse dynamics in the control. It is found that with this biarticular muscle torque, the inertia matrix can be decoupled and has only diagonal elements. Simulation result shows the effectiveness of the proposed control.

I. INTRODUCTION

Development of a robot manipulator that mimics human musculo-skeletal system and analysis of human muscle system have been researched for more than several years. Some researches focus on the measurement of human impedance/stiffness characteristic [1],[2],[3], others focus on the relationship between the stiffness and actual muscle [4],[5].

However, there has been a big distance between these analysis of human muscle system and its application to the control of robot manipulators [6],[7],[8]. This paper develops an analysis methodology and control algorithm that will connect these two systems.

In Section II, the absolute angle Jacobian matrix is shown to be efficient to define the relationship between position/force at the endpoint and three muscle torques. In Section III, the dynamics for three muscles are derived based on the manipulator dynamics. Taking consideration of these two analyses and the characteristic of the pair of muscles, two-degree-of-freedom control is designed for a manipulator with biarticular muscle. Simulation result in Section IV verifies the effectiveness of the proposal.

II. MODIFICATION OF JACOBIAN MATRIX BASED ON BIARTICULAR MUSCLE MODEL

Figure 1 is the configuration of a two degree-of-freedom planar robot manipulator. In order to control the position of the end-effector, the relation between small changes in the position of end-effector and joint angles needs to be defined using the Jacobian matrix described in Equation (1).

Using this Jacobian, the balance between the force applied on the end-effector and the joint torques also can be

S. Oh and Y. Hori is with Department of Electrical Engineering, School of Engineering University of Tokyo, 4-6-1 Komaba Meguroku, Tokyo
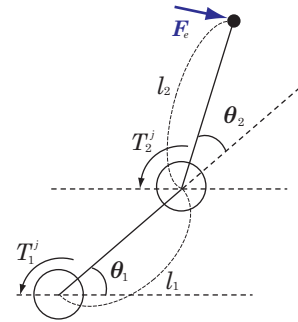sehoon@horilab.iis.u-tokyo.ac.jp

Fig. 1.   Configuration of Two Degree-of-freedom Planar Manipulator

described based on the virtual work principle. Equation (2) is the relationship between the force $\boldsymbol{F}_e$ on the end-effector in Figure 1 and the joint torques (T_1^j, T_2^j); the force $\boldsymbol{F}_e$ in Figure 1 is described as $\boldsymbol{F}_e = (f_x, f_y)^T$.

$$J = \begin{pmatrix} -l_1 \sin\theta_1 - l_2 \sin(\theta_1 + \theta_2) & -l_2 \sin(\theta_1 + \theta_2) \\ l_1 \cos\theta_1 + l_2 \cos(\theta_1 + \theta_2) & l_2 \cos(\theta_1 + \theta_2) \end{pmatrix} \tag{1}$$

$$\begin{pmatrix} T_1^j \\ T_2^j \end{pmatrix} = J^T \begin{pmatrix} f_x \\ f_y \end{pmatrix} \tag{2}$$

A. Jacobian Matrix based on Biarticular Muscle Model

Now, the configuration of a novel manipulator illustrated in Figure 2 is taken into consideration. Biarticular muscle which produces linear force F_m that leads to a torque τ_3^m in two joints is included in this configuration.
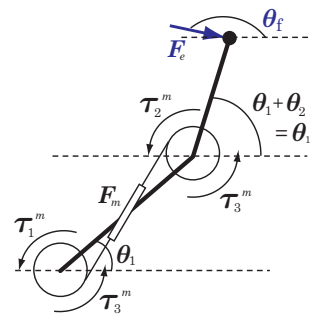

Fig. 2.   Configuration of Two Degree-of-freedom Planar Manipulator with Biarticular Muscle

Actual muscle model has pairs of flexor and extensor muscles; each muscle has its own tension so that two muscles work as a agonistic/antagonistic system. Since the difference between tensions of flexor and extensor muscles work as a

torque at a joint, the outputs of muscles are considered as torques in this paper. τ_1^m, τ_2^m are the torques generated by monoarticular muscles of two joints, and τ_3^m is the torque generated by a biarticular muscle tension F_m. There also is the sum mode in a pair of tensions generated by flexor and extensor muscles. It is true that this conversion to torque cannot reflect this sum mode. The sum mode, however, will be reflected in the feedback control design in the following sections.

The torques generated by these two monoarticular muscles and one biarticular muscle can be projected into the joint torques illustrated in Figure 1. Equation (3) is the relationship.

$$\begin{pmatrix} T_1^j \\ T_2^j \end{pmatrix} = \begin{pmatrix} \tau_1^m + \tau_3^m \\ \tau_2^m + \tau_3^m \end{pmatrix} \quad (3)$$

Note that the torque by the biarticular muscle is added to two joints at the same time.

In order to develop the relationship between the force at the end-effector and the muscle torques, the Jacobian needs to be modified. To this end, we use the relationship between τ_3^m and the absolute angle θ_{12}; the absolute angle $\theta_{12} = \theta_1 + \theta_2$ in Figure 2 can be defined as the output of the biarticular muscle. The point that τ_3^m affects both joints supports this definition, and the dynamics of τ_3^m derived in the following sections also shows this output definition is appropriate.

B. Relationship between Joint/Biarticular Torque and End-point Force

The joint torques related to the end-effector force F_e is distributed to $\tau_1^m, \tau_2^m, \tau_3^m$ in this section. Equation (2) can be divided into two parts like the following equation.

$$J^T \begin{pmatrix} f_x \\ f_y \end{pmatrix} = \begin{pmatrix} -l_1 \sin\theta_1 f_x + l_1 \cos\theta_1 f_y \\ 0 \end{pmatrix} \quad (4)$$
$$+ \begin{pmatrix} -l_2 \sin\theta_{12} f_x + l_2 \cos\theta_{12} f_y \\ -l_2 \sin\theta_{12} f_x + l_2 \cos\theta_{12} f_y \end{pmatrix}$$

Considering this, three muscle torques $\tau_1^m, \tau_2^m, \tau_3^m$ which cope with the external force F_e can be defined as follows.

$$\tau_1^m = -l_1 \sin\theta_1 f_x + l_1 \cos\theta_1 f_y, \quad \tau_2^m = 0 \quad (5)$$
$$\tau_3^m = -l_2 \sin\theta_{12} f_x + l_2 \cos\theta_{12} f_y \quad (6)$$

The muscle torques $\tau_1^m, \tau_2^m, \tau_3^m$ cannot be decided uniquely from the joint torques T_1^j, T_2^j. If, however, we remove τ_2^m intentionally, the relationship can be simplified and it will provide a new relationship between F_e and muscle torques as the following equation.

$$\begin{pmatrix} \tau_1^m \\ \tau_3^m \end{pmatrix} = \begin{pmatrix} 1 & -1 \\ 0 & 1 \end{pmatrix} \begin{pmatrix} T_1^j \\ T_2^j \end{pmatrix}$$
$$= \begin{pmatrix} 1 & -1 \\ 0 & 1 \end{pmatrix} J^T \begin{pmatrix} f_x \\ f_y \end{pmatrix} = (J_{abs})^T \begin{pmatrix} f_x \\ f_y \end{pmatrix}, (7)$$

where J_{abs} stands for the absolute angle Jacobian described as the following equation.

$$J_{abs} = \begin{pmatrix} -l_1 \sin\theta_1 & -l_2 \sin\theta_{12} \\ l_1 \cos\theta_1 & l_2 \cos\theta_{12} \end{pmatrix} = J \begin{pmatrix} 1 & 0 \\ -1 & 1 \end{pmatrix} \quad (8)$$

We found that, with the biarticular muscle, the kinematics can be described by the absolute Jacobian and since the J_{abs} is fit for rotation transformation, the relationship between $\boldsymbol{F}_e$ and $\tau_1^m, \tau_2^m, \tau_3^m$ can be more simplified when $\boldsymbol{F}_e$ are given as $\boldsymbol{F}_e = (F\cos\theta_f, F\sin\theta_f)$.

$$\begin{pmatrix} \tau_1^m \\ \tau_3^m \end{pmatrix} = (J_{abs})^T \begin{pmatrix} F\cos\theta_f \\ F\sin\theta_f \end{pmatrix} = \begin{pmatrix} Fl_1 \sin(\theta_f - \theta_1) \\ Fl_2 \sin(\theta_f - \theta_{12}) \end{pmatrix} \quad (9)$$

Equation (9) is the equation which relates τ_1^m, τ_3^m to the characteristics of the external forces: F and θ_f. With the biarticular muscle torque coordinate, the endpoint force can be designed in a more simple way; two muscle torques are just two functions of $\theta_f, \theta_1, \theta_{12}$ and F.

III. TWO DEGREE OF FREEDOM CONTROL FOR BIARTICULAR MUSCLE MODEL MANIPULATOR

As mentioned previously, there is the sum mode in a muscle pair of flexor and extensor. This section proposes a control design which can realize the difference mode and sum mode of a muscle pair in a robot manipulator, and an impedance control based on a biarticular muscle is suggested.

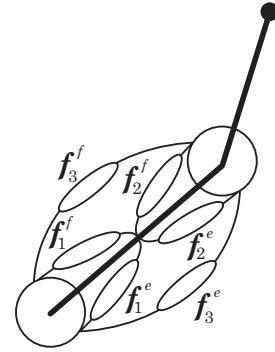*A. Two Degree of Freedom Control Corresponding to Two Modes of Muscle Pair*

Fig. 3. Two-Joint Manipulator with Muscle Model

Figure 3 shows the 3 pairs of muscles: flexors and extensors of two monoarticular muscles and one biarticular muscle. Tension of each flexor and extensor is described as f in this figure. The tensions of flexors and extensors are widely modeled as

$$f^f = u^f - Ku^f r\theta, \quad f^e = u^e + Ku^e r\theta, \quad (10)$$

where u is the contractile force [11]. The sign of the second term changes with regard to the direction a muscle is attached. This tension is reflected to the joint torques as

$$T_1^j = r_1(f_1^f - f_1^e) + r_1(f_3^f - f_3^e) \quad (11)$$
$$= r_1(u_1^f - u_1^e) + r_1(u_3^f - u_3^e) - K_1 r_1(u_1^f + u_1^e)\theta_1$$
$$- K_3 r_1(u_3^f + u_3^e)\theta_1$$
$$T_2^j = r_2(f_2^f - f_2^e) + r_2(f_3^f - f_3^e) \quad (12)$$
$$= r_2(u_2^f - u_2^e) + r_2(u_3^f - u_3^e) - K_2 r_2(u_2^f + u_2^e)\theta_2$$
$$- K_3 r_2(u_3^f + u_3^e)\theta_2,$$

where r_i is the radius of the joint i. In Equations (11) and (12), the first two terms are the difference mode which generates torques to rotate the joints, while the last two terms are the sum mode that is related to the stiffness around the joints.
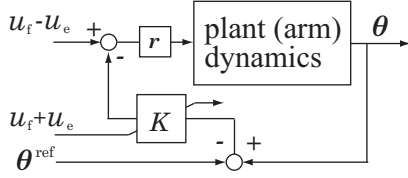

Fig. 4. Illustration of Muscle Input System in a Joint

Figure 4 is the illustration of these roles of two modes in muscle torque; the difference mode working as a torque and the sum mode which adjusts the stiffness.

The virtual trajectory control, which uses the equilibrium point to control the joint angle, also can be represented in this figure. θ^{ref} is the equilibrium point in the virtual trajectory algorithm to control the angle θ. With this designed equilibrium angle θ^{ref} and the designed stiffness K, the angle will converge to θ^{ref}; this is the virtual mode algorithm [9], [10].

Figure 4 provides another insight to the muscle torque input; the difference mode works as feedforward torque input and the sum mode works as feedback gain design, so-called two degree of freedom control. With this new insight, we can recognize that the previous research on muscle driving system focuses more on the feedback characteristics than feedforward characteristics.
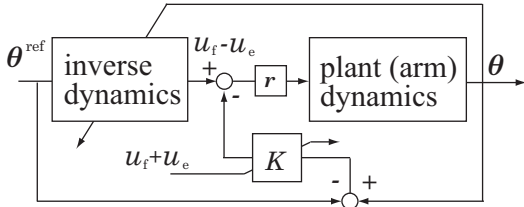

Fig. 5. Feedforward Control for the Difference Mode

For this feedforward torque input design, we suggest an algorithm in Figure 5. Inverse dynamics is adopted to increase the tracking performance. This is old technology in the manipulator control; there have been a number of feedforward controls such as computed torque method so that the suggestion is not new as a control method of manipulator. However this is a new concept as a muscle torque input design. Moreover, we find out that the inverse dynamics can be simplified by diagonalizing the inertia matrix when the biarticular muscle is adopted.

B. Dynamics of Manipulator with Biarticular Muscle Torque Input

Equation (13) shows the dynamics of a robot manipulator, where g is the acceleration of gravity, d_i is the distance from the center of a joint i to the center of the gravity point of the link i, m_i is the weight of the link i, $J_i = m_i d_i^2 + I_i$, and I_i is the moment of inertia about an axis through the center of mass of link i.

$$\begin{pmatrix} J_1+J_2+m_2l_1^2+2m_2l_1d_2\cos\theta_2 & J_2+m_2l_1d_2\cos\theta_2 \\ J_2+m_2l_1d_2\cos\theta_2 & J_2 \end{pmatrix}\begin{pmatrix} \ddot{\theta}_1 \\ \ddot{\theta}_2 \end{pmatrix}$$
$$+\begin{pmatrix} -m_2l_1d_2\sin\theta_2(\dot{\theta}_2^2+2\dot{\theta}_1\dot{\theta}_2) \\ m_2l_1d_2\sin\theta_2\dot{\theta}_1^2 \end{pmatrix}$$
$$+\begin{pmatrix} g(m_1d_1+m_2l_1)\cos\theta_1+gm_2d_2\cos(\theta_1+\theta_2) \\ gm_2d_2\cos(\theta_1+\theta_2) \end{pmatrix}$$
$$=\begin{pmatrix} T_1^j \\ T_2^j \end{pmatrix} \tag{13}$$

Taking the relationship of Equation (3) into consideration, the dynamics of three muscle torques can be derived. We suggest that the dynamics of the biarticular muscle torque is defined as

$$\tau_3^m =$$
$$(J_2+m_2l_1d_2\cos\theta_2)(\ddot{\theta}_1+\ddot{\theta}_2)-m_2l_1d_2\sin\theta_2(\dot{\theta}_2^2+2\dot{\theta}_1\dot{\theta}_2)$$
$$+gm_2d_2\cos(\theta_1+\theta_2). \tag{14}$$

With this dynamics definition, the dynamics for two monoarticular muscle torque is made independent with each other as the following equations.

$$\tau_1^m = (J_1+m_2l_1^2+m_2l_1d_2\cos\theta_2)\ddot{\theta}_1 + g(m_1d_1+m_2l_1)\cos\theta_1 \tag{15}$$
$$\tau_2^m = -m_2l_1d_2\cos\theta_2\ddot{\theta}_2 + m_2l_1d_2\sin\theta_2(\dot{\theta}_1+\dot{\theta}_2)^2 \tag{16}$$

Focusing only on the inertia force terms, we can find that the inertia for each torque is defined without any co-relation with other torques in this dynamics, which means the newly-defined inertia matrix M_{bia} is diagonalized as Equation (17).

$$M_{bia} = \tag{17}$$
$$\begin{pmatrix} J_1+m_2l_1^2+m_2l_1d_2\cos\theta_2 & 0 & 0 \\ 0 & -m_2l_1d_2\cos\theta_2 & 0 \\ 0 & 0 & J_2+m_2l_1d_2\cos\theta_2 \end{pmatrix}$$

Note that the last line of the matrix corresponds to the relationship between the torque τ_3^m and the angle θ_{12}, as we stated previously the angle θ_{12} is the output of the torque τ_3^m. Although the dynamics of $\tau_1^m, \tau_2^m, \tau_3^m$ cannot be determined uniquely, the proposed dynamics can be quite efficient in decoupling the co-relation of joint torques.

We propose to use this dynamics as the inverse dynamics for the feedforward control of each muscle torque so that it can be designed independently. Equations (18) to (20) are the designed feedforward control input for three muscle torques.

$$\tau_1^{m.ff} = \tag{18}$$
$$(J_1+m_2l_1^2+m_2l_1d_2\cos\theta_2)\ddot{\theta}_1^{ref}+g(m_1d_1+m_2l_1)\cos\theta_1$$
$$\tau_2^{m.ff} = \tag{19}$$
$$-m_2l_1d_2\cos\theta_2\ddot{\theta}_2^{ref} + m_2l_1d_2\sin\theta_2(\dot{\theta}_1+\dot{\theta}_2)^2$$
$$\tau_3^{m.ff} = \tag{20}$$
$$(J_2+m_2l_1d_2\cos\theta_2)\ddot{\theta}_{12}^{ref}-m_2l_1d_2\sin\theta_2(\dot{\theta}_2^2+2\dot{\theta}_1\dot{\theta}_2)$$
$$+gm_2d_2\cos\theta_{12}$$

For the disturbance terms, there may be other distribution to $\tau_1^{m.ff}, \tau_2^{m.ff}, \tau_3^{m.ff}$. The proposed feedforward control focuses on decoupling of disturbance; $\tau_1^{m.ff}$ deals with the gravity due to θ_1, $\tau_2^{m.ff}$ deals with the Coriolis force, and disturbance terms assigned on $\tau_3^{m.ff}$ enables this decoupling.

C. Gain Design to Make Arbitrary Endpoint Stiffness

The proposed inverse dynamics will be used for the difference mode of the muscle forces, and as for the design of the sum mode, this section proposes an algorithm to determine the feedback gain K in Figure 5.

The velocity feedback PID control is identified with the impedance force control [12]. The impedance or stiffness control explored in the muscle model researches uses this point as well; with the adjustment of muscle stiffness or position gain in Figure 5, the impedance at the end-effector can be controlled.

With the proposed feedforward position control, this impedance control by feedback gain decision can achieve an excellent hybrid control: feedforward control for a position control and feedback control for force control.

As this feedback force control design, we develop a stiffness ellipse control by determining an appropriate gain of K for muscles. Equation (21) is the stiffness ellipse at the endpoint we want to realize.

$$\left(\begin{array}{c} f_x^e \\ f_y^e \end{array} \right) = \left(\begin{array}{cc} k_1 \cos\theta_e & -k_1 \sin\theta_e \\ k_2 \sin\theta_e & k_2 \cos\theta_e \end{array} \right) \left(\begin{array}{c} \Delta x \\ \Delta y \end{array} \right) \quad (21)$$

When the force $\boldsymbol{F}^e = (f_x^e, f_y^e)$ is applied to the endpoint, the position of the endpoint will change as much as $(\Delta x, \Delta y)$ with this stiffness ellipse design. The tuning parameters in this stiffness ellipse design are k_1, k_2, the major axis and the minor axis, and θ_e, the tilt angle of the ellipse.

The discussion in Section II-A reveals the relationship between this stiffness ellipse and the elasticity, i.e. , the position gain of muscle torques. As with the torque conversion in Section II-A, we design the torque τ_2^m as 0 to make the relationship simple, which simplifies the relationship between the stiffness ellipse matrix in Equation (21) and the gain matrix in Equation (22).

$$\left(\begin{array}{c} \tau_1^{m.fb} \\ \tau_3^{m.fb} \end{array} \right) = \left(\begin{array}{cc} K_1^{bia} & K_2^{bia} \\ K_3^{bia} & K_4^{bia} \end{array} \right) \left(\begin{array}{c} \Delta\theta_1 \\ \Delta\theta_{12} \end{array} \right) \quad (22)$$

In order to derive this gain, $\boldsymbol{F}^e = (f_x^e, f_y^e)$ and $(\Delta x, \Delta y)$ are converted to $\tau_1^m, \tau_2^m, \tau_3^m$ and $\Delta\theta_1, \Delta\theta_{12}$ using the absolute angle Jacobian J_{abs}. Putting the stiffness ellipse in the workspace in Equation (21) as a matrix $\boldsymbol{K}_{ws}$ and using the relationship of Equation (7),the relationship in Equation (22) is represented as follows.

$$\left(\begin{array}{c} \tau_1^{m.fb} \\ \tau_3^{m.fb} \end{array} \right) = \boldsymbol{J}_{abs}^T \boldsymbol{K}_{ws} \boldsymbol{J}_{abs} \left(\begin{array}{c} \Delta\theta_1 \\ \Delta\theta_{12} \end{array} \right) \quad (23)$$

Here we assumed the deviation in the position $(\Delta x, \Delta y)^T$ can be approximated as $\boldsymbol{J}_{abs}(\Delta\theta_1, \Delta\theta_{12})^T$, which means the amount of deviation is small.

One interesting point is that if we divide the workspace stiffness matrix $\boldsymbol{K}_{ws}$ into an axis matrix and a rotation matrix in Equation (24), the rotation angle θ_e can be included in the Jacobian $\boldsymbol{J}_{abs}$.

$$\boldsymbol{K}_{ws}\boldsymbol{J}_{abs}$$
$$= \left(\begin{array}{cc} k_1 & 0 \\ 0 & k_2 \end{array} \right) \left(\begin{array}{cc} \cos\theta_e & -\sin\theta_e \\ \sin\theta_e & \cos\theta_e \end{array} \right) \left(\begin{array}{cc} -l_1\sin\theta_1 & -l_2\sin\theta_{12} \\ l_1\cos\theta_1 & l_2\cos\theta_{12} \end{array} \right)$$
$$= \left(\begin{array}{cc} k_1 & 0 \\ 0 & k_2 \end{array} \right) \left(\begin{array}{cc} -l_1\sin(\theta_1+\theta_e) & -l_2\sin(\theta_{12}+\theta_e) \\ l_1\cos(\theta_1+\theta_e) & l_2\cos(\theta_{12}+\theta_e) \end{array} \right) \quad (24)$$

This rotation in the absolute angle Jacobian results in the following gain decision.

$$K_1^{bia} = l_1^2(k_1\sin\theta_1\sin(\theta_1+\theta_e)+k_2\cos\theta_1\cos(\theta_1+\theta_e)) \quad (25)$$
$$K_2^{bia} = l_1 l_2(k_1\sin\theta_1\sin(\theta_{12}+\theta_e)+k_2\cos\theta_1\cos(\theta_{12}+\theta_e)) \quad (26)$$
$$K_3^{bia} = l_1 l_2(k_1\sin\theta_{12}\sin(\theta_1+\theta_e)+k_2\cos\theta_{12}\cos(\theta_1+\theta_e)) \quad (27)$$
$$K_4^{bia} = l_2^2(k_1\sin\theta_{12}\sin(\theta_{12}+\theta_e)+k_2\cos\theta_{12}\cos(\theta_{12}+\theta_e)) \quad (28)$$

This is the proposed gain decision to achieve the stiffness characteristics at the end-effector. If k_1, k_2, θ_e are specified the gains to realize the stiffness ellipse are determined as above.

Note that the non-diagonal matrix elements K_2^{bia}, K_3^{bia} are not zero in this gain, which means muscle torques τ_1^m, τ_3^m need the angle information of other torque output in order to make the arbitrary stiffness ellipse at the endpoint.

Muscles are said to do a local feedback for its stiffness control; this sharing of the angle information is impossible. To represent this restriction, Equation (29) can be used. This kind of algebraic restriction will result in the directivity of force output at the endpoint in actual muscle.

$$k_1\sin\theta_1\sin(\theta_{12}+\theta_e)+k_2\cos\theta_1\cos(\theta_{12}+\theta_e)$$
$$= k_1\sin\theta_{12}\sin(\theta_1+\theta_e)+k_2\cos\theta_{12}\cos(\theta_1+\theta_e) = 0 \quad (29)$$

To derive more simple condition for this restriction and its comparison with the actual human muscle activity is to be researched.

IV. SIMULATION RESULT

Performance of the proposed muscle torque control is validated by simulations. The proposed control has two degrees of freedom: feedforward control using the proposed inverse dynamics, feedback control using the proposed gain decision algorithm. Equations (18) to (20) are feedforward control input and Equation (23) is feedback control input. For τ_2^m, we only use a feedforward control to keep the stiffness ellipse.

Simulation is performed on a planar manipulator, and the effect of the gravity is ignored. For this reason, the feedforward compensation for the gravity in Equation (18) and (20) are removed.

Figure 6 is the block diagram of simulation. Red line represents the feedforward control, and blue line represents the feedback control. Connection without any sign means the signals are added. Three muscle torques are projected to two joint torque based on Equation (3) and applied to a planar manipulator. Inverse dynamics.1 to 3 adopt the inverse dynamics in Equations (18) to (20). K^{bia} is the gain

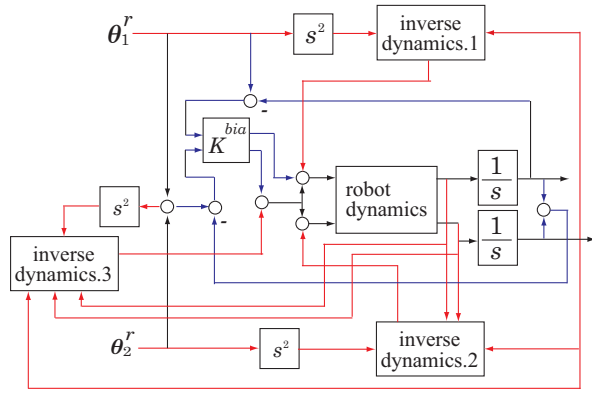Fig. 6. Control Block Diagram for Simulation

we designed in Equations (25) to (28). In addition to the feedback position gain, the velocity of $\dot\theta_1, \dot\theta_{12}$ is fed back to increase damping. The damping gains are set as double of the gain K_{bia}.

In order to validate the fundamental property of the proposed method, no modeling error is considered in this simulation.

A. Tracking Performance by Feedforward Control

First, a sinusoidal wave is added as a reference angle of θ_1. The frequency of the wave will show the performance of reference tracking. 1Hz and 5Hz waves are added. Initial angles of θ_1 and θ_2 is $\theta_1^0 = 0, \theta_2^0 = \frac{\pi}{4}$. Figure 7,8 are the results of θ_1. With high frequency reference, there come
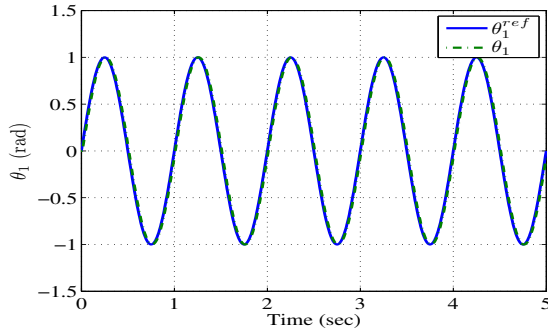

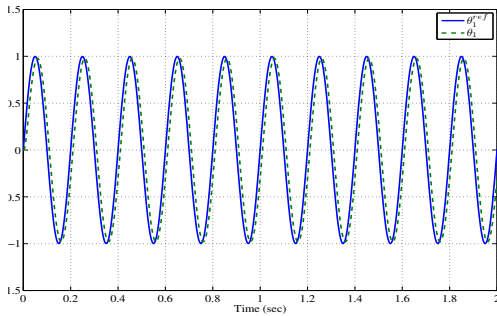Fig. 7. Tracking Performance of θ_1 with 1Hz wave

Fig. 8. Tracking Performance of θ_1 with 5Hz wave

some errors due to the low pass filter in differentiation in the feedforward control.

In actual manipulator control, this kind of time delay is not a problem since the trajectory is designed in a more detailed way. Modeling errors, however, produce these tracking errors. In any case, activated by these errors, the second link also becomes to have errors. Although $\frac{\pi}{4}$ rad is set as a reference angle of θ_2, the actual angle shows the errors in Figures 9 to 10. These errors in θ_1, θ_2 will be
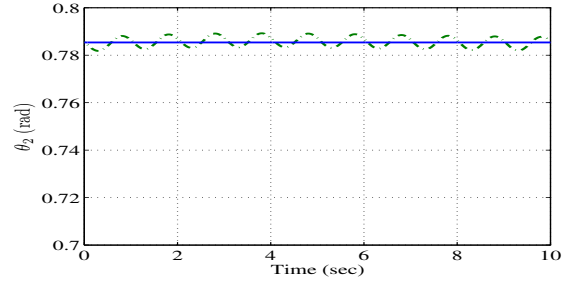

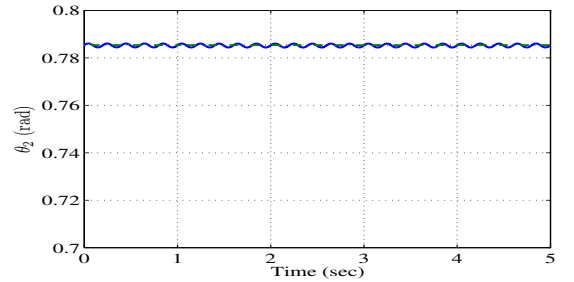Fig. 9. Tracking Performance of θ_2 with 1Hz wave

Fig. 10. Tracking Performance of θ_2 with 5Hz wave

changed according to the gain K^{bia} design.

B. Stiffness Characteristic by Feedback Control

Here, the stiffness characteristic by the proposed feedback control is validated. We will check whether the stiffness in Equation (21) is achieved by the feedback control. Forces (f_x^e, f_y^e) will be applied to the end-effector from various direction, and the derivation of the position $(\Delta x, \Delta y)$ is measured. If the relationship between applied (f_x^e, f_y^e) and measured $(\Delta x, \Delta y)$ is close to Equation (21), the proposed control is proved to be efficient.

Two kinds of $(\Delta x, \Delta y)$ are compared: one is measured $(\Delta x_s, \Delta y_s)$ and the other $(\Delta x_c, \Delta y_c)$ is the values calculated from Equation (21). Simulations are done changing the angle θ_e and the initial angle of θ_2. k_1 and k_2 are set to 10 and 1. The amplitude of the external force F is set constant as $|F_e| = 0.1$, with the angle θ_f in Figure 2 changing. Table I is the simulation result.

The results shows that the stiffness characteristics performed by the proposed feedback control fits well with the stiffness specification given by Equation (21). The errors are caused by the approximation $(\Delta x, \Delta y)^T \simeq \boldsymbol{J}_{abs}(\Delta\theta_1, \Delta\theta_{12})^T$ we used to derive the gain.

TABLE I

COMPARISON OF $(\Delta x, \Delta y)$

Condition	Comparison of Values
$\theta_2^0 = \frac{\pi}{4}, \theta_e = 0, \theta_f = 0$	$\Delta x_s = 0.0091, \Delta y_s = 0.0019$ $\Delta x_c = 0.01, \Delta y_c = 0.0$
$\theta_2^0 = \frac{\pi}{4}, \theta_e = 0, \theta_f = \frac{\pi}{6}$	$\Delta x_s = 0.0043, \Delta y_s = 0.403$ $\Delta x_c = 0.0087, \Delta y_c = 0.050$
$\theta_2^0 = \frac{\pi}{4}, \theta_e = 0, \theta_f = \frac{\pi}{3}$	$\Delta x_s = -0.0042, \Delta y_s = 0.0750$ $\Delta x_c = 0.005, \Delta y_c = 0.0866$
$\theta_2^0 = \frac{\pi}{4}, \theta_e = 0, \theta_f = \frac{\pi}{2}$	$\Delta x_s = -0.0115, \Delta y_s = 0.0940$ $\Delta x_c = 0.0000, \Delta y_c = 0.1000$
$\theta_2^0 = \frac{\pi}{4}, \theta_e = \frac{\pi}{6}, \theta_f = 0$	$\Delta x_s = 0.0078, \Delta y_s = -0.0055$ $\Delta x_c = 0.0087, \Delta y_c = -0.0050$
$\theta_2^0 = \frac{\pi}{4}, \theta_e = \frac{\pi}{6}, \theta_f = \frac{\pi}{6}$	$\Delta x_s = 0.0191, \Delta y_s = 0.0286$ $\Delta x_c = 0.0325, \Delta y_c = 0.0390$
$\theta_2^0 = \frac{\pi}{4}, \theta_e = \frac{\pi}{6}, \theta_f = \frac{\pi}{3}$	$\Delta x_s = 0.0213, \Delta y_s = 0.0565$ $\Delta x_c = 0.0476, \Delta y_c = 0.0725$
$\theta_2^0 = \frac{\pi}{4}, \theta_e = \frac{\pi}{6}, \theta_f = \frac{\pi}{2}$	$\Delta x_s = 0.0196, \Delta y_s = 0.0736$ $\Delta x_c = 0.0500, \Delta y_c = 0.0866$
$\theta_2^0 = \frac{\pi}{4}, \theta_e = \frac{\pi}{3}, \theta_f = 0$	$\Delta x_s = 0.0053, \Delta y_s = -0.0083$ $\Delta x_c = 0.0050, \Delta y_c = -0.0087$
$\theta_2^0 = \frac{\pi}{4}, \theta_e = \frac{\pi}{3}, \theta_f = \frac{\pi}{6}$	$\Delta x_s = 0.0301, \Delta y_s = 0.0121$ $\Delta x_c = 0.0476, \Delta y_c = 0.0175$
$\theta_2^0 = \frac{\pi}{4}, \theta_e = \frac{\pi}{3}, \theta_f = \frac{\pi}{3}$	$\Delta x_s = 0.0402, \Delta y_s = 0.0270$ $\Delta x_c = 0.0775, \Delta y_c = 0.0390$
$\theta_2^0 = \frac{\pi}{4}, \theta_e = \frac{\pi}{3}, \theta_f = \frac{\pi}{2}$	$\Delta x_s = 0.0422, \Delta y_s = 0.0350$ $\Delta x_c = 0.0866, \Delta y_c = 0.0500$
$\theta_2^0 = \frac{\pi}{2}, \theta_e = 0, \theta_f = 0$	$\Delta x_s = 0.0100, \Delta y_s = -0.0002$ $\Delta x_c = 0.0100, \Delta y_c = 0.0000$
$\theta_2^0 = \frac{\pi}{2}, \theta_e = 0, \theta_f = \frac{\pi}{6}$	$\Delta x_s = 0.0064, \Delta y_s = 0.0407$ $\Delta x_c = 0.0087, \Delta y_c = 0.0500$
$\theta_2^0 = \frac{\pi}{2}, \theta_e = 0, \theta_f = \frac{\pi}{3}$	$\Delta x_s = -0.0023 \Delta y_s = 0.0752$ $\Delta x_c = 0.0050, \Delta y_c = 0.0866$
$\theta_2^0 = \frac{\pi}{2}, \theta_e = 0, \theta_f = \frac{\pi}{2}$	$\Delta x_s = -0.0117, \Delta y_s = 0.0962$ $\Delta x_c = 0.0000, \Delta y_c = 0.1000$
$\theta_2^0 = \frac{\pi}{2}, \theta_e = \frac{\pi}{6}, \theta_f = 0$	$\Delta x_s = 0.0091, \Delta y_s = -0.0042$ $\Delta x_c = 0.0087, \Delta y_c = -0.0050$
$\theta_2^0 = \frac{\pi}{2}, \theta_e = \frac{\pi}{6}, \theta_f = \frac{\pi}{6}$	$\Delta x_s = 0.0270, \Delta y_s = 0.0315$ $\Delta x_c = 0.0325, \Delta y_c = 0.0390$
$\theta_2^0 = \frac{\pi}{2}, \theta_e = \frac{\pi}{6}, \theta_f = \frac{\pi}{3}$	$\Delta x_s = 0.0365, \Delta y_s = 0.0476$ $\Delta x_c = 0.0476, \Delta y_c = 0.0725$
$\theta_2^0 = \frac{\pi}{2}, \theta_e = \frac{\pi}{6}, \theta_f = \frac{\pi}{2}$	$\Delta x_s = 0.0382, \Delta y_s = 0.0810$ $\Delta x_c = 0.0500, \Delta y_c = 0.0866$
$\theta_2^0 = \frac{\pi}{2}, \theta_e = \frac{\pi}{3}, \theta_f = 0$	$\Delta x_s = 0.0066, \Delta y_s = -0.0078$ $\Delta x_c = 0.0050, \Delta y_c = -0.0087$
$\theta_2^0 = \frac{\pi}{2}, \theta_e = \frac{\pi}{3}, \theta_f = \frac{\pi}{6}$	$\Delta x_s = 0.0436, \Delta y_s = 0.0132$ $\Delta x_c = 0.0476, \Delta y_c = 0.0175$
$\theta_2^0 = \frac{\pi}{2}, \theta_e = \frac{\pi}{3}, \theta_f = \frac{\pi}{3}$	$\Delta x_s = 0.0694, \Delta y_s = 0.0297$ $\Delta x_c = 0.0775, \Delta y_c = 0.0390$
$\theta_2^0 = \frac{\pi}{2}, \theta_e = \frac{\pi}{3}, \theta_f = \frac{\pi}{2}$	$\Delta x_s = 0.0800, \Delta y_s = 0.0400$ $\Delta x_c = 0.0866, \Delta y_c = 0.0500$

V. CONCLUSIONS AND FUTURE WORKS

A. Conclusions

This paper proposed a feedforward control and feedback control for a manipulator which has a biarticular muscle torque. For this development, we showed that the absolute angle Jacobian matrix is efficient in deriving the relationship between the position/force at the endpoint and the three muscle torques.

We also focused on two modes of agonistic/antagonistic muscles: the sum mode and the difference mode in a pair of muscles, and developed a feedforward control for the difference mode and a feedback control for the sum mode. We derived inverse dynamics for three muscle torques and

used it for the feedforward control of three muscle torques. The proposed dynamics has a diagonalized inertia matrix; the biarticular muscle decouples the conventional inertia matrix.

As for the feedback control, a methodology to determine the gain based on the stiffness ellipse at the workspace was suggested. Simulation result verified the performance of the proposed control design: fast position tracking and stiffness ellipse characteristics were achieved successfully.

B. Future Works

The proposed control design still needs angle information of other joint, and thus it requires some modification to be independent control of muscles; the diagonalized inertia matrix still has the angle θ_2 in all elements, which can be solved if θ_2 is given in a feedforward way, not feedback from the real angle. Restriction of the stiffness ellipse specification in Equation (21) is necessary for the independent control. Equation (29) can be a hint to this restriction.

The proposed control does not include a feedback control of τ_2^m. If we can design a feedback control that is quite robust to external forces such as the disturbance observer, the errors of θ_2 in Figure 9 and 10 can be attenuated. Development a robot that has a biarticular muscle torque and experiment using the robot is our future work.

REFERENCES

[1] D. W. Franklin, G. Liaw, T. E. Milner, R. Osu, E. Burdet, M. Kawato, "Endpoint Stiffness of the Arm Is Directionally Tuned to Instability in the Environment", *Journal of Neuroscience*, vol. 27(29), 2007, pp. 7705-7716

[2] S. Stroeve, "Impedance Characteristics of a Neuromuscluloskeletal Model of the Human Arm I. Posture Control", *Biological Cybernetics*, vol. 81, 1999, pp.475-494.

[3] F. Flash, F. Mussa-Ivaldi, "Human Arm Stiffness Characteristics during the Maintenance of Posture", *Experimental Brain Research*, vol. 82, 1990, pp. 315-326.

[4] K. Tahara, Z. Luo, S. Arimoto, "On Control Mechanism of Human-Like Reaching Movements with Musculo-Skeletal Redundancy", *Proc. of IEEE/RSJ Int'l Conference on Intelligent Robots and Systems*, 2006, pp.1402-1409

[5] H. Gomi, M. Kawato, "Task-Dependent Viscoelasticity of Human Multijoint Arm and Its Spatial Characteristics for Interaction with Environments", *Journal of Neuroscience*, vol. 18(21), 1998, pp. 8965-8978.

[6] N. Hogan, "Impedance Control: An Approach to manipulation: Part II - Implementation", *Journal of Dynamic Systems, Measurement, and Control*, vol. 107, 1985, pp. 8-16.

[7] M. Kumamoto, T. Oshima, T. Yamamoto, "Control Properties Induced by the Existence of Antagonistic Pairs of Bi-articular Muscles - Mechanical Engineering Model Analyses", *Human Movement Science*, vol. 13, 1994, pp. 611-634.

[8] K. Yoshida, T. Uchida, Y. Hori, "Novel FF Control Algorithm of Robot Arm Based on Bi-articular Muscle Principle - Emulation of Muscular Viscoelasticity for Disturbance Suppression and Path Tracking", *Proc. of IEEE IECON*, 2007, pp.310-315

[9] M. Katayama, M. Kawato, "Virtual Trajectory and stiffness ellipse during multijoint arm movement predicted by neural inverse model", *Biological Cybernetics*, vol. 69, 1993, pp. 353-362.

[10] H. Gomi, M. Kawato, "Human Arm Stiffness and Equilibrium-point Trajectory during Multi-Joint Movement", *Biological Cybernetics*, vol. 76, 1997, pp. 163-171.

[11] K. Ito, T. Tsuji, "The Bilinear Characteristics of Muscle-skeleto Motor System and the Application to Prosthesis Control", *Trans. of IEEJ*, vol. 105-C, 1985, pp. 201-208. (in Japanese)

[12] S. Oh, Y. Hori, "Generalized discussion on design of force-sensor-less Power Assist Control", *Proc. IEEE International Workshop on Advanced Motion Control*, 2008. pp.492-497